Figure S1

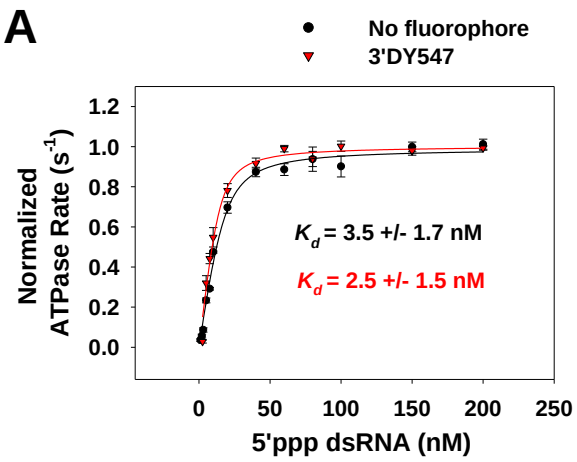
A
No fluorophore
3'DY547
Normalized ATPase Rate (s^{-1})
K_d = 3.5 +/- 1.7 nM
K_d = 2.5 +/- 1.5 nM
5'ppp dsRNA (nM)

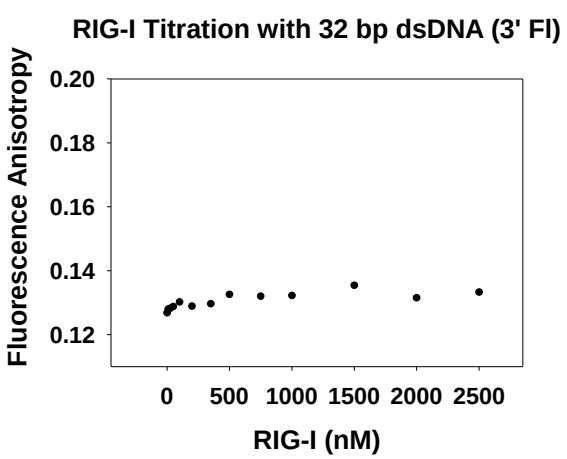
B
RIG-I Titration with 32 bp dsDNA (3' Fl)
Fluorescence Anisotropy
RIG-I (nM)

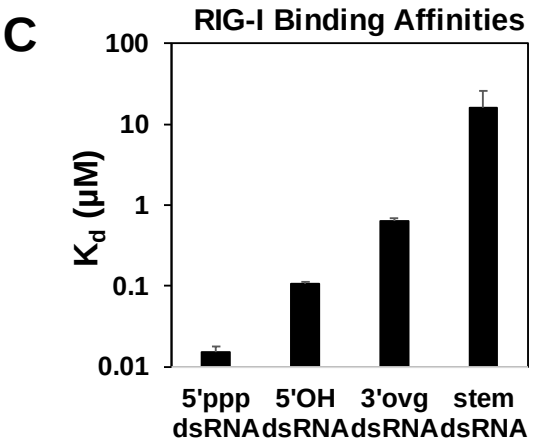
C
RIG-I Binding Affinities
K_d (μM)
5'ppp dsRNA
5'OH dsRNA
3'ovg dsRNA
stem dsRNA

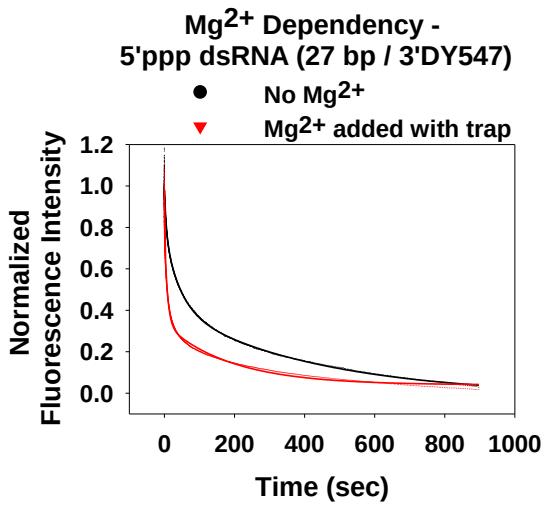
D
Mg^{2+} Dependency -
5'ppp dsRNA (27 bp / 3'DY547)
No Mg^{2+}
Mg^{2+} added with trap
Normalized Fluorescence Intensity
Time (sec)

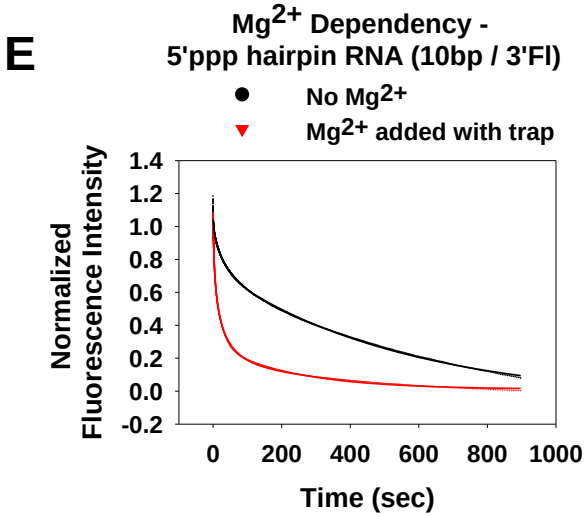
E
Mg^{2+} Dependency -
5'ppp hairpin RNA (10bp / 3'Fl)
No Mg^{2+}
Mg^{2+} added with trap
Normalized Fluorescence Intensity
Time (sec)

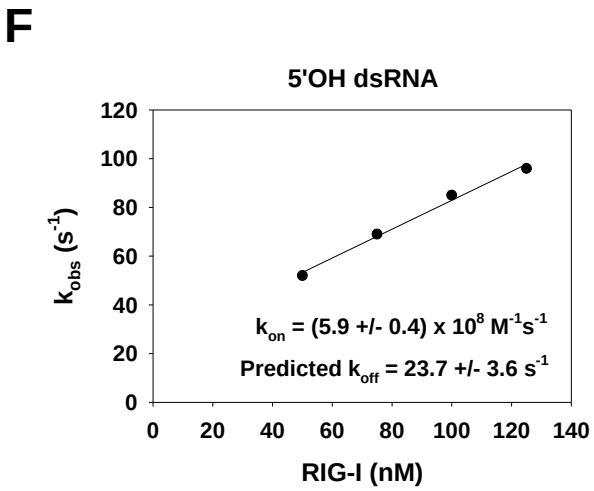
F
5'OH dsRNA
k_{obs} (s^{-1})
k_{on} = (5.9 +/- 0.4) x 10^8 $M^{-1}s^{-1}$
Predicted k_{off} = 23.7 +/- 3.6 s^{-1}
RIG-I (nM)

Figure S1 (related to Figure 1): RIG-I activation pathway and bimolecular on-rate constants of RIG-I and RD for 5'ppp and non-PAMP dsRNA. (A) The K_d values of unlabeled 5'ppp dsRNA (black) and 3'DY547 labeled 5'ppp dsRNA (red) were measured by titrating RIG-I (10 nM) with increasing concentrations of RNA in Buffer A with 1 mM ATP at 25^{o}C, and then measuring the ATPase activity by the radiometric assay. (B) A 3'-fluorescein labeled 32-bp DNA (20 nM) was titrated with increasing concentrations of RIG-I and fluorescence anisotropy was recorded at 25^{o}C. The data shows no binding of RIG-I to the DNA. (C) Fluorescence intensity based K_d titrations of RIG-I with a dsRNA panel (Figure 1B) were carried out at 25^{o}C and the values are presented in a bar chart form. (D-E) Off-rate kinetics of RIG-I (15 nM) from the DY547-labeled 27 bp 5'ppp dsRNA (20 nM) (D) and 3'-fluorescein-labeled 10 bp 5'ppp hairpin RNA (20 nM) (E) in absence and presence of Mg^{2+} (3 mM) are shown. Preformed equimolar complexes of RIG-I and the specified dsRNA were mixed with a 10-fold excess of trap (5'ppp hairpin RNA, non-fluorescent) in Buffer A without Mg^{2+} (black) or in Buffer A with Mg^{2+} (red) at 25^{o}C. The traces were fit to a sum of two exponentials and the average lifetime of RIG-I complex on the 27 bp 5'ppp dsRNA is ~120 sec in the absence of Mg^{2+} and ~60 sec in the presence of Mg^{2+}. A similar analysis showed that the average lifetime of RIG-I complex on the 10 bp 5'ppp hairpin RNA is ~325 sec in the absence of Mg^{2+} and ~45 sec in the presence of Mg^{2+}. (F) Representative plot showing a linear increase in the observed rates of RIG-I binding to the 5'OH dsRNA. RIG-I (45 to 200 nM) was mixed with 10 nM of 5'OH dsRNA and the increase in fluorescence intensity with time was fit to a single exponential to obtain the observed rates of RNA binding shown on the y-axis. The slope provides the on-rate and the intercept the off-rate, which matched the experimentally measured off-rates.

Figure S2

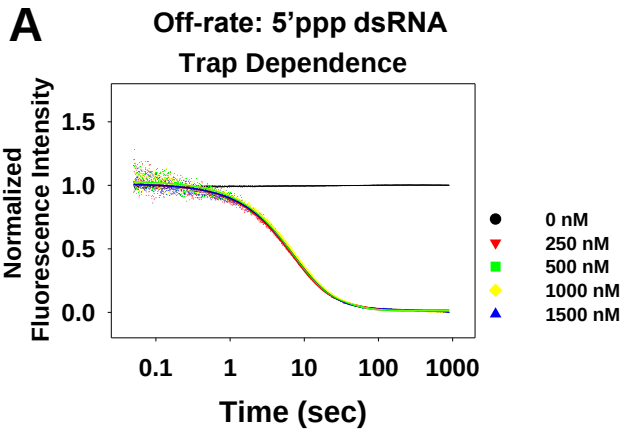
A
Off-rate: 5'ppp dsRNA
Trap Dependence
Normalized Fluorescence Intensity
1.5
1.0
0.5
0.0
0.1
1
10
100
1000
Time (sec)
0 nM
250 nM
500 nM
1000 nM
1500 nM

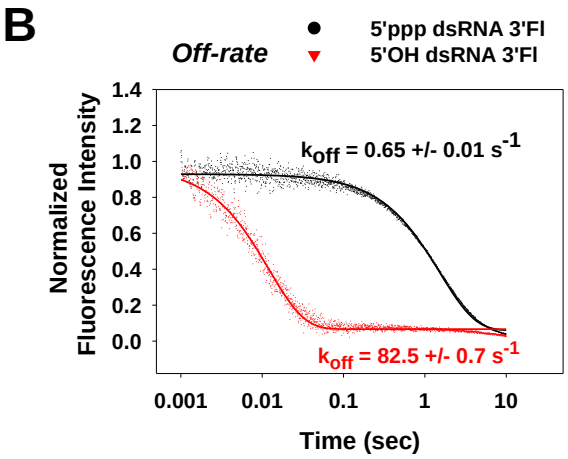
B
Off-rate
5'ppp dsRNA 3'Fl
5'OH dsRNA 3'Fl
Normalized Fluorescence Intensity
1.4
1.2
1.0
0.8
0.6
0.4
0.2
0.0
koff = 0.65 +/- 0.01 s-1
koff = 82.5 +/- 0.7 s-1
0.001
0.01
0.1
1
10
Time (sec)

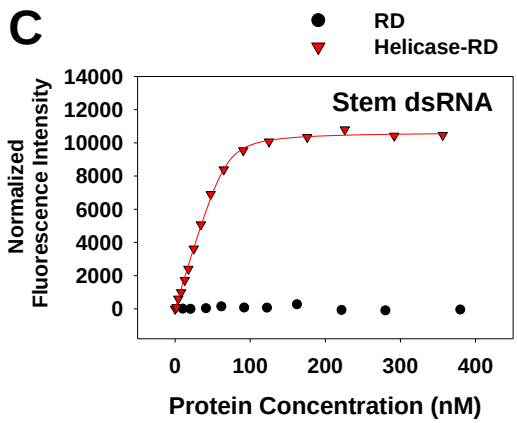
C
RD
Helicase-RD
Stem dsRNA
Normalized Fluorescence Intensity
14000
12000
10000
8000
6000
4000
2000
0
0
100
200
300
400
Protein Concentration (nM)

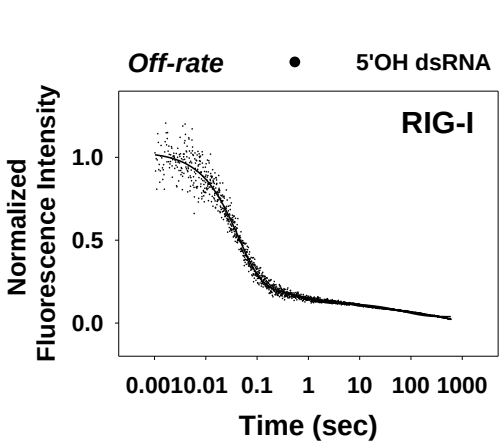
D
Off-rate
5'OH dsRNA
RIG-I
Normalized Fluorescence Intensity
1.0
0.5
0.0
0.0010.01
0.1
1
10
100
1000
Time (sec)

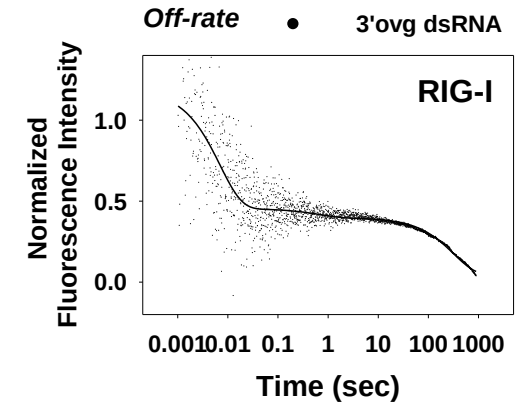
E
Off-rate
3'ovg dsRNA
RIG-I
Normalized Fluorescence Intensity
1.0
0.5
0.0
0.0010.01
0.1
1
10
100
1000
Time (sec)

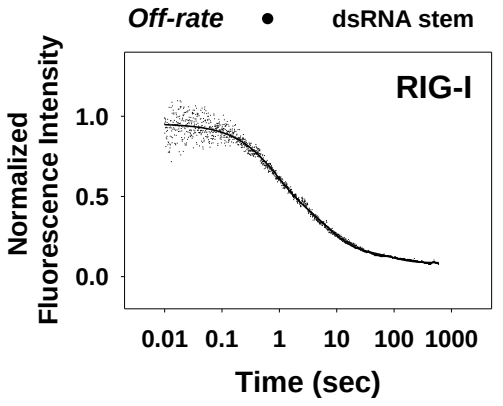
F
Off-rate
dsRNA stem
RIG-I
Normalized Fluorescence Intensity
1.0
0.5
0.0
0.01
0.1
1
10
100
1000
Time (sec)

Figure S2 (related to Figure 2): Off-rate constants of 5’ppp and non-PAMP RNAs from RD, Helicase-RD, and RIG-I. (A) Stopped-flow off-rate kinetics of RIG-I (50 nM) from Dy547-labeled 5’ppp dsRNA (50 nM) in presence of ATP (2 mM) and increasing concentrations of trap (5’ppp 12bp hairpin RNA) were measured at 25^{o}C and the respective fluorescence traces are shown. (B) Off-rate kinetics of RD (50 nM) from 3’ fluorescein labelled 5’ppp and 5’OH dsRNA (50 nM) at 25^{o}C are shown and the respective off-rates are listed. The fold difference between fluorescein labeled 5’ppp and 5’OH dsRNA off-rates is similar to their DY547 tagged versions. (C) A fluorescence intensity based titration of RD (black) and Helicase-RD (red) with Cy3 labeled stem dsRNA (20 nM) is shown. (D-F) Off-rate kinetics of RIG-I from fluorophore-labeled 5’OH dsRNA (D), 3’ovg dsRNA (E) and stem dsRNA (F) were measured in Buffer A at 25^{o}C. A preformed complex of RIG-I with the specified fluorophore tagged RNA was chased with a 10-fold excess of unlabeled 5’ppp ds12 hairpin RNA. The concentrations are listed in the methods section. The solid lines are fit to single exponential or sum of two or three exponentials that provided the off-rates listed in Table S1. The presented traces are an average of 4-6 individual traces.

Figure S3

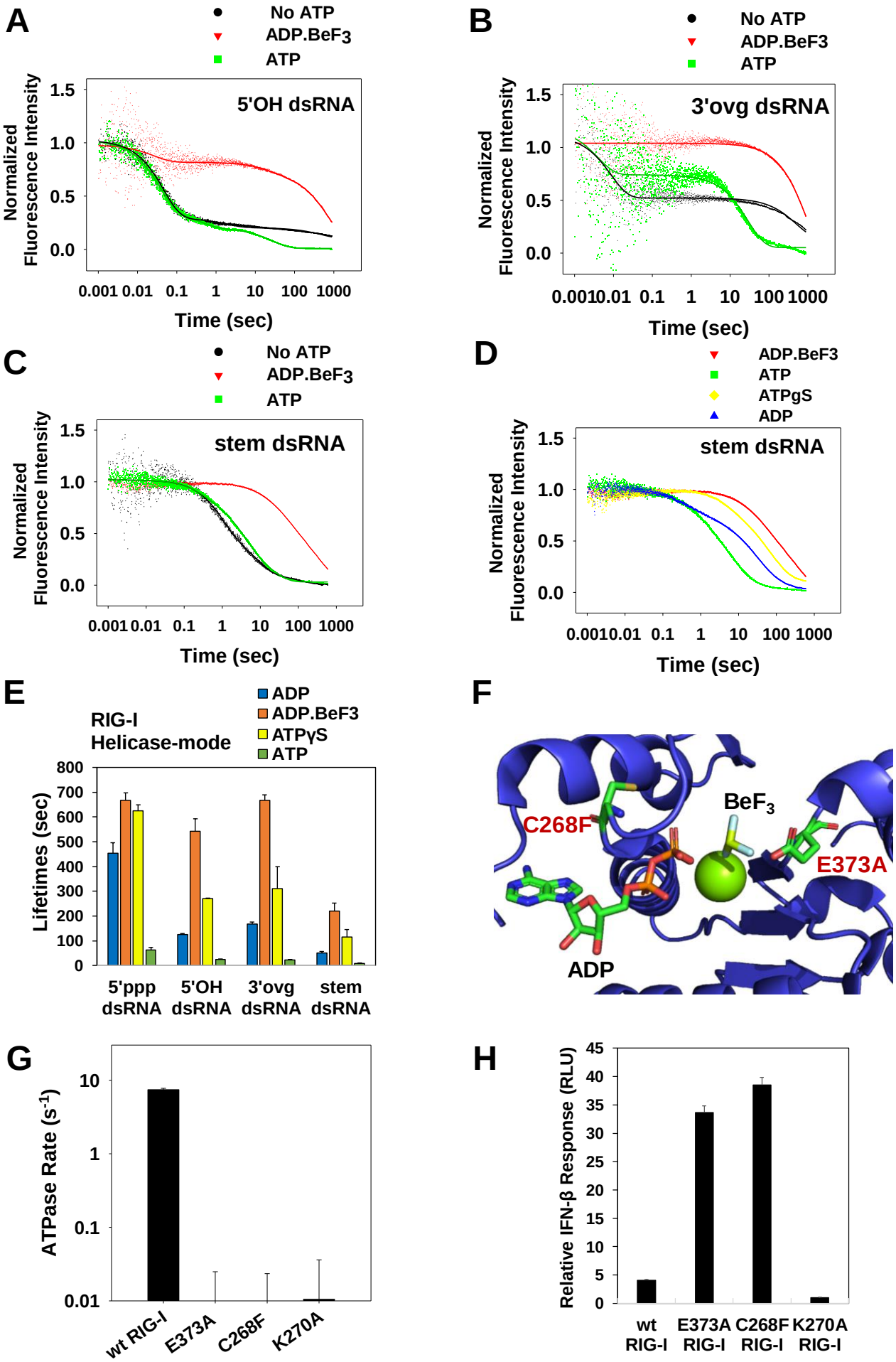
A
No ATP
ADP.BeF3
ATP
5'OH dsRNA
Normalized Fluorescence Intensity
Time (sec)
B
No ATP
ADP.BeF3
ATP
3'ovg dsRNA
Normalized Fluorescence Intensity
Time (sec)
C
No ATP
ADP.BeF3
ATP
stem dsRNA
Normalized Fluorescence Intensity
Time (sec)
D
ADP.BeF3
ATP
ATPgS
ADP
stem dsRNA
Normalized Fluorescence Intensity
Time (sec)
E
RIG-I
Helicase-mode
ADP
ADP.BeF3
ATPγS
ATP
Lifetimes (sec)
5'ppp dsRNA
5'OH dsRNA
3'ovg dsRNA
stem dsRNA
F
BeF3
C268F
E373A
ADP
G
ATPase Rate (s-1)
wt RIG-I
E373A
C268F
K270A
H
Relative IFN-β Response (RLU)
wt RIG-I
E373A RIG-I
C268F RIG-I
K270A RIG-I

Figure S3 (related to Figure 3): Off-rate constants of 5'ppp and non-PAMP RNAs from RIG-I and SMS mutants in the presence of ATP and ATP analogs. (A-D) Representative stopped-flow kinetic traces show the off-rate kinetics of RIG-I from DY547-labeled 5'OH dsRNA (A), 3'ovg dsRNA (B) and Cy3 labeled stem dsRNA (C,D) under the specified nucleotide conditions in Buffer A at 25^{o}C. The dissociation kinetics were fit to two or three exponentials to estimate the off-rates, and lifetimes of the RD-mode and Helicase-mode populations were determined from the off-rates. The experimental concentrations are listed in the methods section. (E) The lifetimes of RIG-I Helicase-mode populations for the specified dsRNAs and ATP analogs are presented in a bar chart form. (F) A magnified view of the catalytic residues of RIG-I and the bound ATP analog (ADP.BeF_3) (PDB ID: 5E3H). The two mutations associated with atypical Singleton Merton Syndrome, E373A and C268F are highlighted. (G) The steady-state ATPase rates of wild-type, E373A, C268F and K270A RIG-I (10 nM) with 5'ppp dsRNA (1 μM) were measured using 1 mM ATP at 25^{o}C in Buffer A. (H) Interferon-β (IFN-β) reporter activation in HEK293T cells expressing wild-type, E373A, C268F and K270A RIG-I in the absence of any transfected ligand is shown. Error bars are SEM from quadruplicate sets.

Figure S4

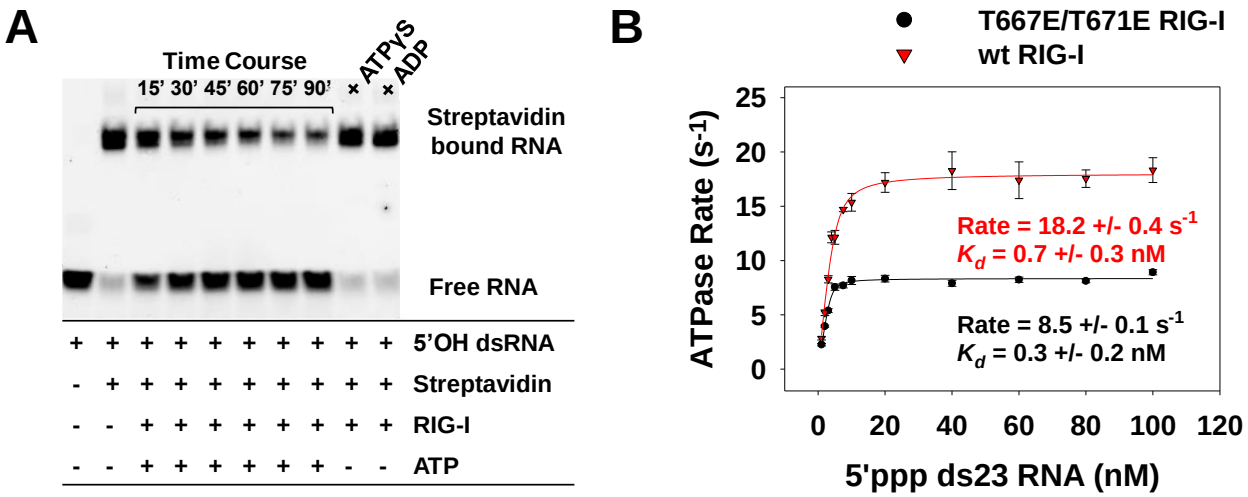

Figure S4 (related to Figure 4): Directionality of RIG-I translocation and role of Helicase motif IVa. (A) The 4-20% TBE gel scan shows a time-course of biotin-streptavidin displacement on 5'OH dsRNA by RIG-I at 25°C in Buffer A without nucleotide or ATP, ATPγS, or ADP. A preformed complex of 5'OH dsRNA (25 nM) conjugated to monovalent streptavidin (60 nM) and RIG-I (25 nM) was mixed with ATP/ATP analog (1 mM) and free biotin (50 µM) to start the time-course. (B) An ATPase based titration (radiometric) of T667E/T671E RIG-I (black) and wild-type RIG-I (red) (10 nM) with increasing 5'ppp dsRNA (23 bp) in Buffer A with 1 mM ATP at 37°C is shown, and the respective K_d and ATPase rates are listed.

Figure S5

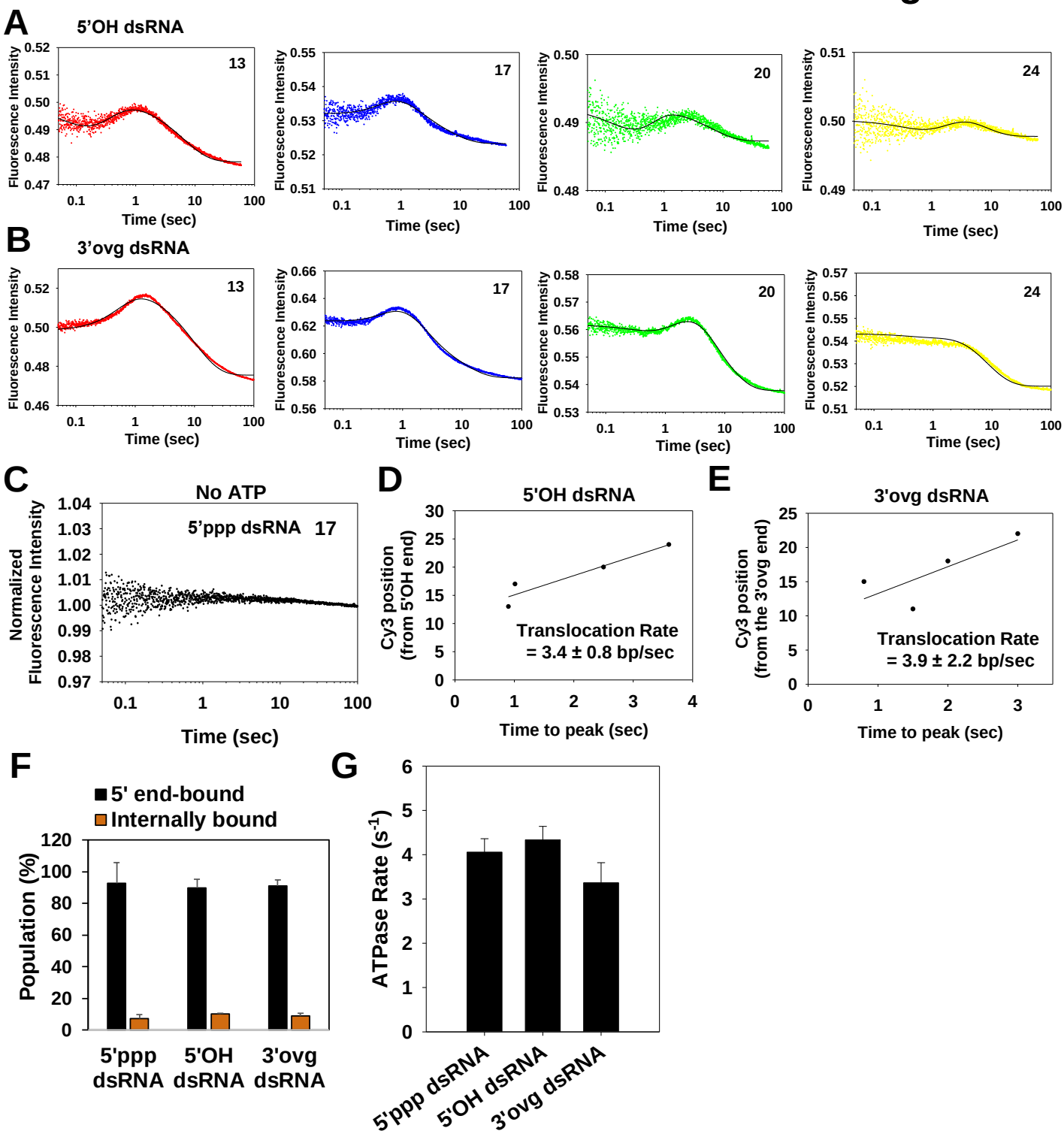
A
5'OH dsRNA
13
17
20
24
Fluorescence Intensity
Time (sec)
B
3'ovg dsRNA
13
17
20
24
Fluorescence Intensity
Time (sec)
C
No ATP
5'ppp dsRNA 17
Normalized Fluorescence Intensity
Time (sec)
D
5'OH dsRNA
Cy3 position (from 5'OH end)
Translocation Rate = 3.4 ± 0.8 bp/sec
Time to peak (sec)
E
3'ovg dsRNA
Cy3 position (from the 3'ovg end)
Translocation Rate = 3.9 ± 2.2 bp/sec
Time to peak (sec)
F
5' end-bound
Internally bound
Population (%)
5'ppp dsRNA
5'OH dsRNA
3'ovg dsRNA
G
ATPase Rate (s^{-1})
5'ppp dsRNA
5'OH dsRNA
3'ovg dsRNA

Figure S5 (related to Figure 5): Fluorescence stopped-flow assay measures the stepping rates of RIG-I translocation (A-B) Time courses of Cy3 fluorescence intensity changes measure the transient state kinetics of RIG-I translocation on the 5'OH dsRNA (A) and 3'ovg dsRNA (B). The number on the upper-right corner specifies the Cy3 fluorophore position from the RNA-end. Experiments were conduced by mixing a preformed complex of RIG-I (50 nM) and the specified dsRNA (75 nM) from one syringe with 2 mM ATP and 10-fold excess of unlabeled 5'ppp ds12 hairpin RNA (trap) from the other syringe in Buffer A at 25^{o}C. (C) Time-course of Cy3 fluorescence intensity change after rapid mixing of RIG-I (20 nM) and 5'ppp dsRNA carrying internal Cy3 (30 nM) (17th bp from 5'ppp) in absence of ATP is shown. (D-E) Time-to-peak analysis of data in A-B provides the average translocation rate of RIG-I on the 5'OH dsRNA (D) and 3'ovg dsRNA (E). (F) The fluorescence intensity time-courses in A-B and Figure 5B-E were fit to a minimal model shown in Figure 5G using Kintek Explorer. The percentage of RNA-end bound RIG-I versus RIG-I bound internally in RNA at the fluorophore positions was estimated from the best fit. (G) The steady-state ATPase rates of wild-type RIG-I (10 nM) for the specified dsRNA (1 µM) were measured with 2 mM ATP at 25^{o}C in Buffer A using the radiometric assay.

Figure S6

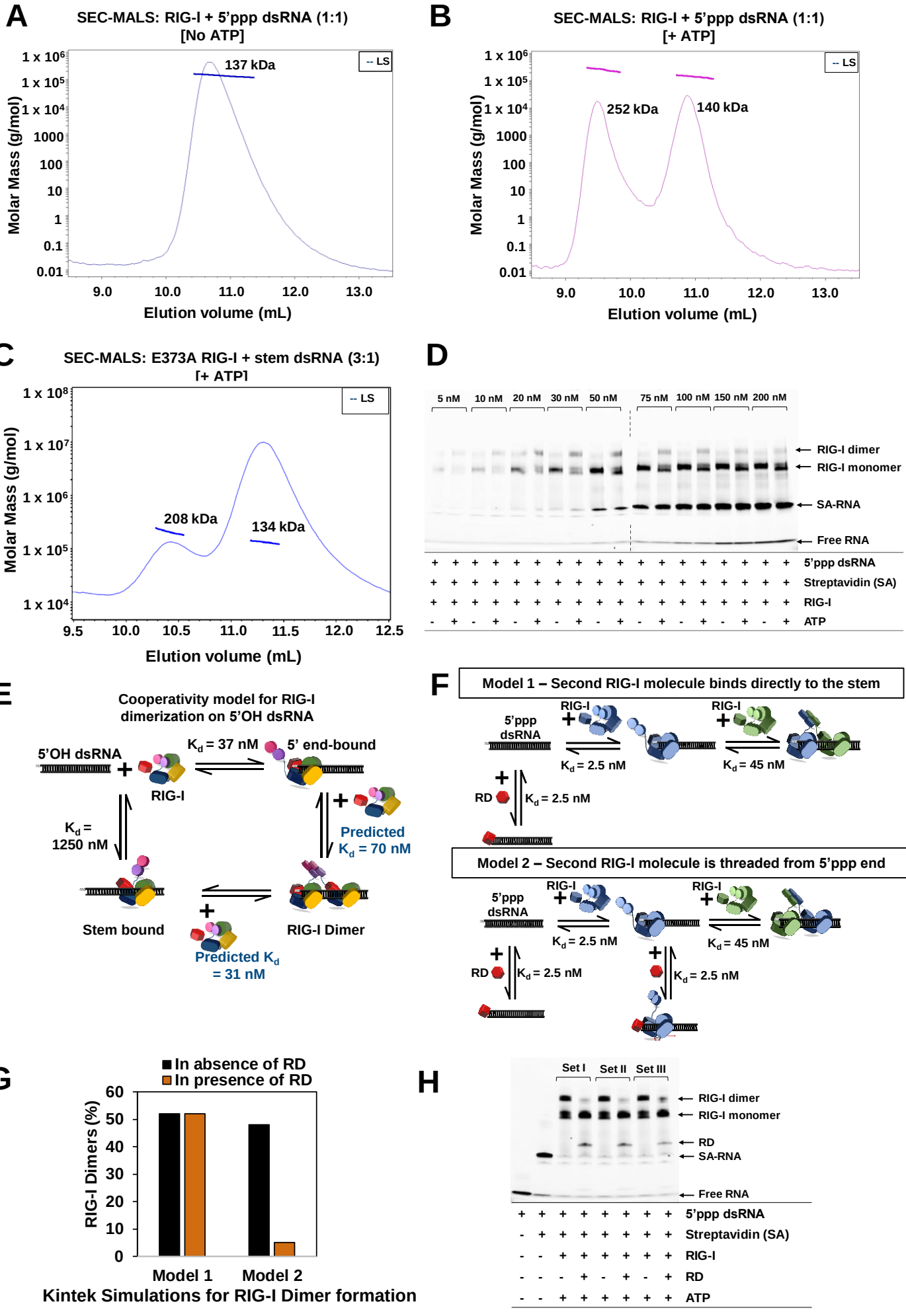
A
SEC-MALS: RIG-I + 5'ppp dsRNA (1:1)
[No ATP]
137 kDa
-- LS
Molar Mass (g/mol)
Elution volume (mL)
B
SEC-MALS: RIG-I + 5'ppp dsRNA (1:1)
[+ ATP]
252 kDa
140 kDa
-- LS
Molar Mass (g/mol)
Elution volume (mL)
C
SEC-MALS: E373A RIG-I + stem dsRNA (3:1)
[+ ATP]
208 kDa
134 kDa
-- LS
Molar Mass (g/mol)
Elution volume (mL)
D
5 nM
10 nM
20 nM
30 nM
50 nM
75 nM
100 nM
150 nM
200 nM
RIG-I dimer
RIG-I monomer
SA-RNA
Free RNA
5'ppp dsRNA
Streptavidin (SA)
RIG-I
ATP
E
Cooperativity model for RIG-I
dimerization on 5'OH dsRNA
5'OH dsRNA
RIG-I
Kd = 37 nM
5' end-bound
Kd =
1250 nM
Predicted
Kd = 70 nM
Stem bound
RIG-I Dimer
Predicted Kd
= 31 nM
F
Model 1 – Second RIG-I molecule binds directly to the stem
5'ppp
dsRNA
RIG-I
Kd = 2.5 nM
RIG-I
Kd = 45 nM
RD
Kd = 2.5 nM
Model 2 – Second RIG-I molecule is threaded from 5'ppp end
5'ppp
dsRNA
RIG-I
Kd = 2.5 nM
RIG-I
Kd = 45 nM
RD
Kd = 2.5 nM
Kd = 2.5 nM
G
In absence of RD
In presence of RD
RIG-I Dimers (%)
Model 1
Model 2
Kintek Simulations for RIG-I Dimer formation
H
Set I
Set II
Set III
RIG-I dimer
RIG-I monomer
RD
SA-RNA
Free RNA
5'ppp dsRNA
Streptavidin (SA)
RIG-I
RD
ATP

Figure S6 (related to Figure 6): ATP facilitates cooperative RIG-I dimerization on 5'ppp dsRNA by a 5'-end threading mechanism. (A-B) The light scattering profile from a SEC-MALS experiment of RIG-I and 5'ppp dsRNA under 1:1 stoichiometry (7.5 µM) in absence of ATP (A), and in presence of ATP (3 mM) (B) is shown. The predicted molecular mass is listed. For (A): 137±2 kDa and for (B): 252±8 kDa and 140±3 kDa. Experimental details outlined in the methods section. (C) A complex of E373A RIG-I (7.5 µM) and stem dsRNA (20bp RNA flanked by 4bp DNA and 5'ovg, 2.5 µM) (3:1) in presence of ATP was analyzed by SEC-MALS. The light scattering profiles of the monomer and dimer peak are shown and the predicted molecular mass is listed (208±4 kDa and 134±2 kDa). Experimental details outlined in the methods section. (D) RIG-I (50 nM) was titrated with increasing concentrations (5-200 nM) of DY547-labeled 5'ppp dsRNA in the presence of ATP (2 mM), and EMSA was used to calculate percent RIG-I dimers. (E) A dimerization model was constructed with the measured K_d values of RIG-I complexes on the 5'OH dsRNA-end and stem (values in black text). The dimerization data from 5'OH dsRNA titration, similar to (D), was used to fit to this model and the predicted K_d values for the second RIG-I molecule are presented in blue. (F-G) Kintek explorer was used to simulate two models of RIG-I dimerization and RD was used as a competitor for testing these models (F). The expected results from model simulations with the given K_d values of each species under conditions of 75 nM RIG-I, 75 nM RD, and 25 nM RNA are presented in (G). (H) EMSA of DY547-labeled 5'ppp dsRNA (25 nM) and RIG-I (75 nM) incubated with ATP (2 mM), in presence or absence of RD (75 nM) is shown. The experiments were done in triplicates.

Table S1

	RD (s^{-1})	Helicase-RD (s^{-1})	RIG-I	
			RD-mode (s^{-1})	Helicase-mode (s^{-1})
5'ppp dsRNA	0.14 ± 0.03 (100%)	0.0022 ± 0.0001 (100%)	0.15 ± 0.02 (70%)	0.0025 ± 0.0008 (30%)
5'OH dsRNA	25 ± 0.7 (100%)	0.1 ± 0.004 (29%) and 0.003 ± 0.0001 (71%)	21 ± 1 (86%)	0.12 ± 0.01 (7%) and 0.003 ± 0.0004 (7%)
3'ovg dsRNA	120 ± 7.7 (100%)	0.07 ± 0.002 (24%) and 0.003 ± 0.0001 (76%)	125 ± 23 (67%)	0.04 ± 0.01 (4%) and 0.003 ± 0.0001 (29%)
stem dsRNA	-	1.7 ± 0.23 (11%), 0.07 ± 0.005 (41%) and 0.01 ± 0.0006 (48%)	-	1.4 ± 0.06 (46%), 0.17 ± 0.009 (42%) and 0.02 ± 0.002 (12%)

Table S1 *(related to Figure 2)*: Off-rate constants of 5'ppp and non-PAMP RNAs from RD, Helicase-RD, and RIG-I. The dissociation kinetics of RD, Helicase-RD and wt RIG-I-RNA complexes were analyzed and the observed populations, their respective dissociation rates and their percent contribution in the total complex are presented in a tabular format.

Table S2

	No ATP (s^{-1})		ADP.BeF_3 (s^{-1})		ATP (s^{-1})	
	RD-mode	**Helicase-mode**	**RD-mode**	**Helicase-mode**	**RD-mode**	**Helicase-mode**
5'ppp dsRNA	0.15 ± 0.02 (71%)	0.0025 ± 0.0008 (29%)	0.1 ± 0.002 (55%)	0.0015 ± 0.0007 (45%)	0.12 ± 0.005 (58%)	0.016 ± 0.002 (42%)
5'OH dsRNA	21 ± 1 (85%)	0.12 ± 0.01 (7%) and 0.003 ± 0.0004 (8%)	25 ± 2 (16%)	0.058 ± 0.005 (11%) and 0.0016 ± 0.0005 (73%)	25 ± 1.4 (52%)	0.04 ± 0.003 (48%)
3'ovg dsRNA	125 ± 23 (61%)	0.004 ± 0.001 (39%)	-	0.0015 ± 0.0005 (100%)	128 ± 17 (40%)	0.044 ± 0.005 (60%)
stem dsRNA	-	1.4 ± 0.06 (46%), 0.17 ± 0.009 (42%) and 0.02 ± 0.002 (12%)	-	0.028 ± 0.001 (38%) and 0.004 ± 0.0002 (62%)	-	1.5 ± 0.04 (21%), 0.18 ± 0.004 (64%) and 0.03 ± 0.001 (15%)

Table S2 (r*elated to Figure 3)*: Off-rate constants of 5'ppp and non-PAMP RNAs from RIG-I in absence or presence of ATP/ATP analog. The dissociation kinetics of RIG-I-RNA complexes in the absence or presence of ATP and ATP analogs were analyzed and the observed populations and their respective dissociation rates are presented in a tabular format.

Table S3

	No ATP (nM)	ADP.BeF_3 (nM)	ATP (nM)
5'ppp dsRNA	12 ± 1.5	38 ± 2.5	2.5 ± 1.5
5'OH dsRNA	85 ± 6	160 ± 8	37 ± 4
3'ovg dsRNA	600 ± 40	265 ± 21	50 ± 18
stem dsRNA	16000 ± 9800	2200 ± 175	1250 ± 160

Table S3 (*related to Figure 3). Equilibrium binding affinities of RIG-I for PAMP and non-PAMP RNAs.* The binding affinities of RIG-I for the specified RNAs were measured in the absence or presence of ATP and ATP analogs and the measured K_d values are presented in a tabular format.

Table S4

	E373A RIG-I (nM)	C268F RIG-I (nM)
5’ppp dsRNA	12 ± 2	15 ± 3
5'OH dsRNA	31 ± 1	34 ± 8
3'ovg dsRNA	68 ± 5	98 ± 10
stem dsRNA	500 ± 40	925 ± 73

Table S4 (*Related to Figure 3). Equilibrium binding affinities of E373A and C268F RIG-I for PAMP and non-PAMP RNAs.* The binding affinities of E373A and C268F RIG-I for the specified RNAs were measured in the presence of ATP using fluorescence intensity titrations, and the measured K_d values are presented in a tabular format.

Table S5

	No ATP			ATP		
	RD-mode (s^{-1})	**Helicase-mode (s^{-1})**	**Helicase-mode Lifetime (sec)**	**RD-mode (s^{-1})**	**Helicase-mode (s^{-1})**	**Helicase-mode Lifetime (sec)**
5'ppp dsRNA	0.13 ± 0.001 (82%)	0.004 ± 0.0001 (18%)	250 ± 11.5	0.1 ± 0.001 (52%)	0.002 ± 0.0002 (48%)	500 ± 55
5'OH dsRNA	20 ± 1.1 (46%)	0.07 ± 0.002 (18%) and 0.005 ± 0.0001 (36%)	135 ± 5	19 ± 4 (7%)	0.06 ± 0.001 (28%) and 0.0024 ± 0.0005 (65%)	294 ± 8
3'ovg dsRNA	110 ± 21 (30%)	0.14 ± 0.01 (25%) and 0.004 ± 0.0002 (45%)	150 ± 9	-	0.032 ± 0.002 (33%) and 0.003 ± 0.0002 (67%)	266 ± 26
stem dsRNA	-	6.4 ± 0.3 (39%), 0.44 ± 0.03 (39%) and 0.014 ± 0.003 (22%)	8.8 ± 0.8	-	0.03 ± 0.0006 (23%) and 0.003 ± 0.00003 (77%)	228 ± 5

Table S5 (*related to Figure 3).* Off-rate constants of 5'ppp and non-PAMP RNAs from E373A RIG-I in absence or presence of ATP. The dissociation kinetics of E373A RIG-I with the specified RNA in the absence or presence of ATP were fit to a sum of two or three exponentials and the observed populations, their respective dissociation rates and the helicase-mode lifetimes are presented in a tabular format.

Table S6

	No ATP			ATP		
	RD-mode (s^{-1})	**Helicase-mode (s^{-1})**	**Helicase-mode Lifetime (sec)**	**RD-mode (s^{-1})**	**Helicase-mode (s^{-1})**	**Helicase-mode Lifetime (sec)**
5'ppp dsRNA	0.13 ± 0.002 (50%)	0.03 ± 0.001 (27%) and 0.002 ± 0.0001 (23%)	150 ± 7	0.12 ± 0.001 (51%)	0.028 ± 0.001 (27%) and 0.002 ± 0.0001 (22%)	133 ± 7
5'OH dsRNA	17 ± 2.8 (19%)	0.07 ± 0.002 (21%) and 0.003 ± 0.0001 (60%)	200 ± 6.8	17 ± 3 (13%)	0.14 ± 0.003 (22%) and 0.0034 ± 0.0001 (65%)	194 ± 6.5
3'ovg dsRNA	-	0.05 ± 0.002 (30%) and 0.002 ± 0.0001 (70%)	254 ± 18	-	0.04 ± 0.001 (29%) and 0.002 ± 0.0001 (71%)	248 ± 11
stem dsRNA	-	0.06 ± 0.003 (36%), 0.014 ± 0.002 (27%) and 0.005 ± 0.0001 (37%)	96 ± 40	-	0.11 ± 0.004 (31%), 0.017 ± 0.002 (41%) and 0.005 ± 0.0008 (29%)	84 ± 17

Table S6 (*Related to Figure 3).* Off-rate constants of 5'ppp and non-PAMP RNAs from C268F RIG-I in absence or presence of ATP. The dissociation kinetics of C268F RIG-I with the specified RNA in the absence or presence of ATP were fit to a sum of two or three exponentials and the observed populations, their respective dissociation rates and the helicase-mode lifetimes are presented in a tabular format.

Table S7

Rates (s^{-1})	5’ppp dsRNA	5’OH dsRNA	3’ovg dsRNA
k_1	0.028 ± 0.003	0.11 ± 0.004	0.1 ± 0.002
k_2	0.54 ± 0.05	3.2 ± 0.12	2.5 ± 0.1
k_3	1.8 ± 0.6	4.4 ± 0.14	4.2 ± 0.2
k_4	1.1 ± 0.2	6.9 ± 0.3	4.1 ± 0.1
k_5	1.25 ± 0.2	15 ± 1	5.5 ± 0.2
k_6	0.32 ± 0.05	6.2 ± 0.4	4.4 ± 0.3
k_7	0.08 ± 0.29	1 ± 0.1	0.5 ± 0.04
k_8	0.13 ± 0.09	2.3 ± 0.2	1.3 ± 0.07
k_9	0.68 ± 0.8	1.7 ± 0.2	1 ± 0.05

Table S7 (r*elated to Figure 5). Global data fitting of RIG-I translocation assays.* The fluorescent traces from the stopped-flow translocation assays were fit to a minimal 5-step model (Figure 5G) using the Kintek Explorer software and the individual rates for the 5 steps for 5’ppp, 5’OH and 3’ovg dsRNA as well as the rates of dissociation of RIG-I prebound at the 4 fluorophore positions are presented in a tabular format.